

Study of the In-Plane Anisotropy in a Co/Cu/Co Trilayer

R. A. Sukhachev^{a, *} and M. V. Mamonova^a

^a Dostoevsky Omsk State University, Omsk, 644077 Russia

*e-mail: sukhachevruslan@gmail.com

Received May 22, 2023; revised June 19, 2023; accepted July 28, 2023

Abstract—Magnetic characteristics of Co films on a surface of Cu are calculated numerically within the spin density functional theory. The energy efficiency of the antiferromagnetic and ferromagnetic configurations at different layer thicknesses is studied. The magnetic moments of atoms, and the energy and parameter of the magnetic anisotropy of the Co/Cu/Co structure are determined with allowance for spin–orbit coupling, depending on the orientation of the surface’s face.

Keywords: magnetic anisotropy, ultrathin magnetic films

DOI: 10.3103/S1062873823703835

INTRODUCTION

The magnetism of thin films is an important area of research with a special impact on technological progress. Such materials find wide application in spintronic, nanoelectronic, and microelectronic devices. They are used in particular to store and record information in memory devices, ensuring a high density and speed of recording information [1].

Researchers’ interest in this area is due to its results contributing greatly to the development of physics of magnetism [2] by studying such intriguing effects as giant magnetoresistance [3].

One of the most important physical properties affecting magnetic microstructure, magnetization switching, and other magnetic characteristics is magnetic anisotropy. Its existence in the Co/Cu/Co system has been discussed in many studies [4–7]. Bulk Co has high Curie temperature $T_C = 1388$ K [8], making this material promising for use at room temperature, plus a strong single-ion anisotropy with a mag-

netic anisotropy energy of $E_{MA} = 655 \frac{\mu\text{eV}}{\text{atom}}$ [9] and a

magnetic moment of $\mu = 1.73 \frac{\mu_B}{\text{atom}}$ [9]. It was shown experimentally in [4] that cobalt films exhibit in-plane uniaxial anisotropy with an easy magnetization axis, since they lack the strong positive surface anisotropy that would allow magnetization to align perpendicular to the surface. Perpendicular magnetic anisotropy in Co/Cu is consequently less widely studied [5]. Kohlhepp et al. [6] and den Broeder et al. [7] confirmed that the Co/Cu(111) system displays weak perpendicular anisotropy.

Since the mutual orientation of magnetic moments of different layers depends on the spacings between them, it is important to predict theoretically at which thickness of a nonmagnetic layer will a certain magnetic configuration be more energetically advantageous. The magnetic moments of a Co/Cu/Co structure obtained in some works [10, 11] also depend on the thickness of the nonmagnetic layer, as was shown in [8], where the magnetization of the system changed as the thickness of copper spacers was varied from 2 to 15 Å.

The aim of this work was to study the magnetic characteristics of the Co/Cu/Co system at different thicknesses of the nonmagnetic layer and cobalt films. We calculated the effect the surface orientation has on the energy of magnetic anisotropy and obtained the relationship between the thickness of the cobalt magnetic layer and the parameter of magnetic anisotropy. The contribution from the energy of magnetocrystalline anisotropy (MCA) induced by spin–orbit coupling to the energy of magnetic anisotropy was also examined.

The calculations in this work were made using the VASP package, one of the most common and efficient software tools for calculating the electronic structure of many-particle systems in quantum physics and quantum chemistry. It is based on the spin density functional theory, within which the total energy is calculated as the electron density functional minimum using the generalized gradient approximation (GGA) for the energy of exchange correlation and projective augmented waves (PAW). This makes the approach preferable for use in numerical calculations. To allow calculation of the magnetic properties, the energy of the system is written as a functional of the densities of electrons and magnetization, which are calculated

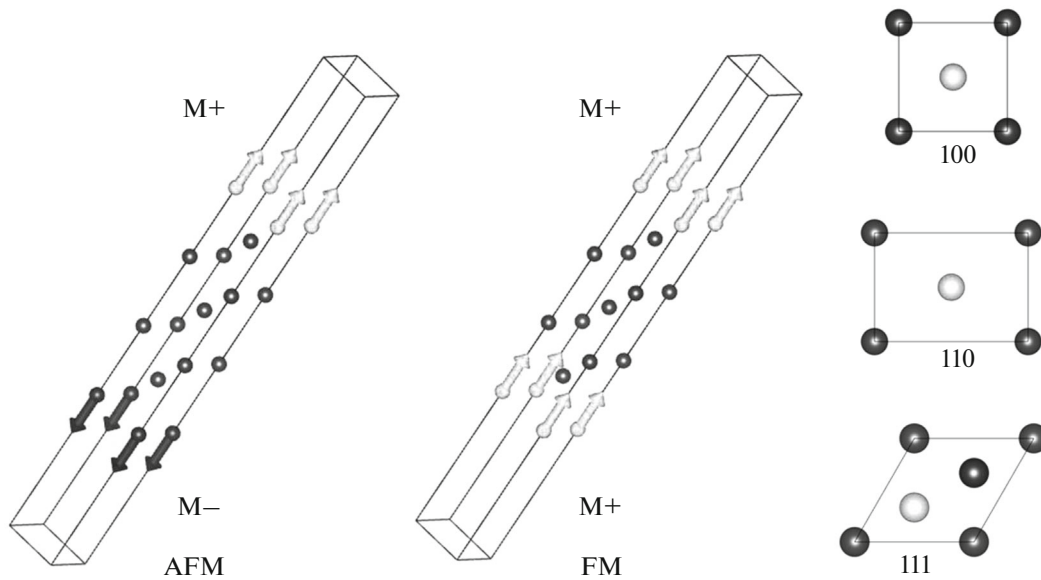


Fig. 1. Crystal structure of surface cells and a supercell with the orientation of the magnetic moments of atoms.

self-consistently and depend on the magnetic moment of each atom in the system. Magnetization was considered in two versions: collinear, where the magnetic moment is specified by a scalar quantity, and noncollinear, where the magnetic moment is specified by a vector. We investigated two magnetic configurations of the Co/Cu/Co system (Fig. 1): antiferromagnetic (AFM), where the magnetic moments of atoms in films on both sides of the spacer are directed opposite to each other, and ferromagnetic (FM) when they are co-directional.

These states differ in the established order of the magnetic moments of atoms or ions. In antiferromagnets, the spin magnetic moments of electrons are spontaneously aligned antiparallel to each other. Antiferromagnets therefore have very low magnetic susceptibility and behave like weak paramagnets. In contrast, the magnetic moments of atoms in ferromagnets are parallel to each other. At temperatures below the Curie point, they can be magnetized without an external magnetic field.

Table 1. Difference between the total energy of a supercell in a trilayer system with the AFM and FM configurations at different layer thicknesses

N_{Cu}	$\Delta E (N_{\text{Co}} = 1),$ meV	$\Delta E (N_{\text{Co}} = 2),$ meV	$\Delta E (N_{\text{Co}} = 3),$ meV
3	7.102	3.710	3.561
5	-3.142	-2.709	0.059
7	-4.033	5.460	-3.196
9	-3.747	-0.864	318.548

Another important feature of the system is the geometry of the surface (i.e., the type of the modeled surface cell and the position of the adsorbed atom). Examples of surface geometry can be seen in Fig. 1 with faces (100), (110), and (111). These faces have a number of features. Surface (111) of copper is the one most densely packed and stable. Surface (100) is a square lattice obtained by splitting a face-centered bulk plane. Surface (110) is the least stable of the investigated surfaces [12].

Collinear calculations were made ignoring the spin-orbit coupling within which the magnetic moments were obtained. We studied the energy advantage of the system's spin configurations, which can be defined as $\Delta E = E_{\text{AFM}} - E_{\text{FM}}$ (i.e., the difference between the total energies of the AFM and FM configurations). The total energies of a supercell with one atom in the layer were obtained (Fig. 1). The number of nonmagnetic (copper) spacer layers was taken to be 3, 5, 7, and 9 at cobalt film thicknesses of 1–3 monolayers. The size of the k grid used in our calculations was $48 \times 48 \times 1$, and the cutoff energy was $E_{\text{cut}} = 600$ eV. The ΔE values calculated for face (100) of the surface are listed in Table 1.

Based on the above data, which show the dependence of the energy difference between AFM and FM structures of one supercell atom on a substrate and the thickness of the magnetic material, we can reach the following conclusions. The FM configuration becomes more energetically advantageous at three cobalt monolayers and five and nine substrate layers (approximately 0.7 and 1.6 nm, respectively). The AFM configuration is favored at a copper thickness of 7 monolayers (approximately 1.0 nm). These results are confirmed by the experimental work of another

Table 2. Magnetic moments of individual atoms in the Co/Cu/Co system

N_{Cu}	$\mu(N_{\text{Co}} = 1), \mu\text{B}$		$\mu(N_{\text{Co}} = 2), \mu\text{B}$		$\mu(N_{\text{Co}} = 3), \mu\text{B}$	
	AFM	FM	AFM	FM	AFM	FM
3	-1.865	1.866	-1.599	1.598	-1.660	1.670
			-1.790	1.789	-1.644	1.652
					-1.877	1.876
5	-1.868	1.863	-1.603	1.594	-1.655	1.665
			-1.789	1.785	-1.656	1.651
					-1.872	1.872
7	-1.865	1.866	-1.594	1.593	-1.657	1.659
			-1.782	1.781	-1.652	1.652
					-1.876	1.877
9	-1.867	1.866	-1.596	1.598	0.318	1.658
			-1.786	1.784	-1.520	1.650
					-1.861	1.883

team [13–15]. The AFM configuration is favored in the structure consisting of a single cobalt and copper monolayer five to nine monolayers thick. An advantageous FM configuration in a system consisting of two cobalt monolayers is seven copper monolayers. Advantageous AFM configurations are five and nine copper monolayers. Table 2 gives the magnetic moments of cobalt atoms for the investigated configurations. We can see the magnetic moments depend weakly on the spin configurations: the difference is $\sim 0.01 \mu\text{B}$. The largest magnetic moment corresponds to the cobalt atom farthest from the spacer.

Table 3 gives the reduced magnetic moment (i.e., the ratio between the total magnetic moment of the system and the number of atoms of the magnetic material) for an FM configuration with 7 monolayers of a nonmagnetic (copper) spacer, depending on the number of ferromagnet (cobalt) layers.

The calculated magnetic moments agree well with the experimental data obtained by other researchers.

A collinear system was calculated earlier that had no preferred axis of magnetization along which magnetic moments could be directed. However, this must be done to study features of noncollinear magnetism, particularly the properties of magnetic anisotropy determined by the dependence of the system's magnetic properties on the direction of magnetization with respect to the structural axes of the crystal that form it. We are interested in directions x and z (i.e., in the plane of the film and perpendicular to it).

Table 4 gives calculated energies $E_{\text{MA}} = E_{\perp} - E_{\parallel}$ of magnetic anisotropy, depending on the surface orientation, which can be defined as the difference between the total energies of the system at the magnetic moments directed in the plane of the film (E_{\parallel}) and perpendicular to it (E_{\perp}).

Table 3. Average magnetic moment, depending on cobalt film thickness. N_{Co} is the number of Co monolayers, μ_{tot}^1 is the value obtained in calculations, and μ_{tot}^2 is a magnetic moment borrowed from the experimental work of other researchers

System	N_{Co}	$\mu_{\text{tot}}^1, \mu\text{B}/\text{atom}$	$\mu_{\text{tot}}^2, \mu\text{B}/\text{atom}$
Co/Cu/Co	1	1.826	2.111 [16]
			1.901 [11]
			1.891 [17]
	2	1.691	1.73 [4]
			1.74 [18]
			2.1(3) [19]
	3	1.715	1.81 [20]

They showed that the configuration with magnetic moments parallel to the plane of the film was energetically more advantageous for faces (100) and (111), which is in good agreement with data from other researchers [6, 21]. The existence of the vanishingly weak anisotropy found experimentally in [22] was confirmed for face (110).

Table 4. Total supercell energies and magnetic moments of atoms in the 1Co/3Cu/1Co system for faces (100), (110), and (111)

Face	E_{\parallel}, eV	E_{\perp}, eV	$E_{\text{MA}}, \text{meV}$	$\mu, \mu\text{B}$
100	-22.717 099	-22.716 201	0.898	1.870
				1.863
110	-21.663 702	-21.663 726	-0.024	1.730
				1.866
111	-23.282 756	-23.281 794	0.961	1.756
				1.752

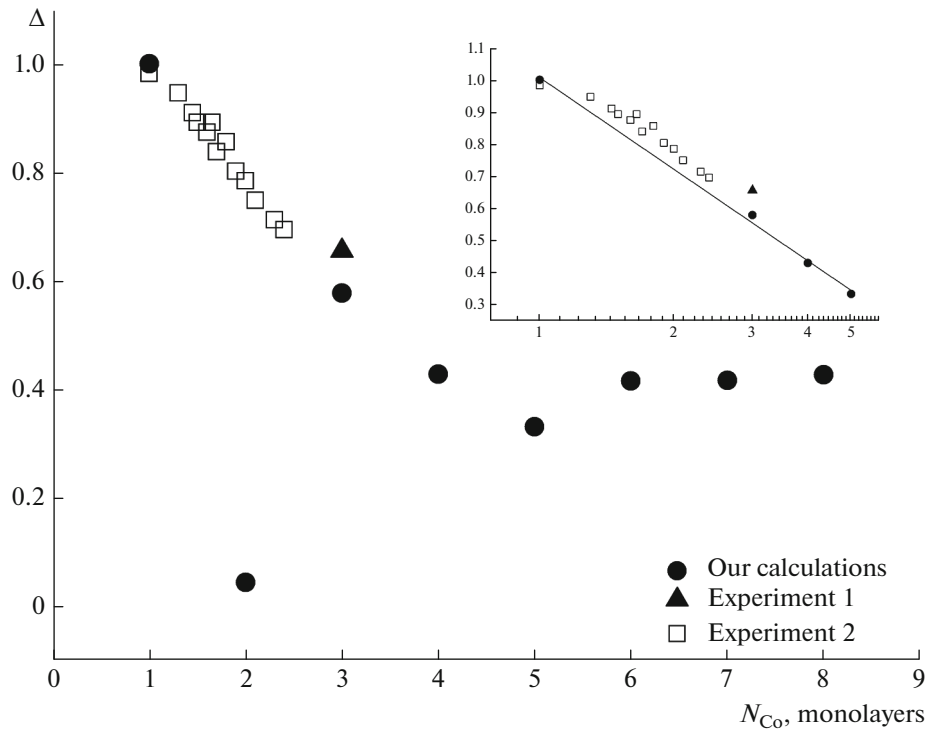


Fig. 2. Calculated parameters of anisotropy, depending on the number of cobalt monolayers relative to values $\Delta = 1 - \frac{T_c(N)}{T_c(\infty)}$ obtained in $T_c(N)$ experiments with Co/Cu(100) (Experiment 1) [23] and (Experiment 2) [24]). The inset in the main plot is an approximation of the parameters of magnetic anisotropy, depending on the number of cobalt monolayers on a logarithmic scale.

For numerical Monte Carlo modeling [2] and comparing our results to experiments, we must know the type of anisotropy and the parameter of anisotropy in the Hamiltonian of a system with anisotropy

$$H_{\parallel} = -\sum_{i,j} J_{i,j} \{S_i^x S_j^x + S_i^y S_j^y + (1 - \Delta_{\parallel}) S_i^z S_j^z\}. \quad (1)$$

Let us find the dependence of parameter Δ_{\parallel} of magnetic anisotropy on the number of layers of our magnetic material (cobalt).

Table 5. Average magnetic moment of the Co/Cu system at different directions of magnetization: in film plane (\parallel) and perpendicular to it (\perp)

N_{Co}	$\mu_{tot}, \mu B/atom$	
	\parallel	\perp
1	1.879	1.878
2	1.692	1.692
3	1.729	1.729
4	1.689	1.691
5	1.697	1.698
6	1.687	1.687
7	1.686	1.686
8	1.684	1.684

Let all spins be directed along the x axis. We then have $S_i^x = S_j^x = S$; $S_i^y = S_j^y = 0$; $S_i^z = S_j^z = 0$. We substitute these values into (1) and obtain

$$E_{\parallel} = -\sum_{i,j} J_{i,j} S^2. \quad (2)$$

We now direct spins along axis z . After similar actions, we arrive at

$$E_{\perp} = -\sum_{i,j} J_{i,j} S^2 (1 - \Delta_{\parallel}). \quad (3)$$

Let us derive the parameter of anisotropy from the obtained equations:

$$E_{\parallel} < E_{\perp} \Rightarrow \Delta_{\parallel} = \frac{E_{\parallel} - E_{\perp}}{E_{\parallel}}. \quad (4)$$

The ferromagnetic configuration of the system for face (100) was calculated at a constant copper thickness of 3 monolayers and cobalt thicknesses of 1 to 8 monolayers.

Figure 2 compares the calculated parameters of anisotropy to values $\Delta = 1 - \frac{T_c(N)}{T_c(\infty)}$, obtained from experimental critical temperatures $T_c(N)$ for Co/Cu(100) [23, 24] depending on the number of

Table 6. Energies of spin–orbit coupling at different directions of magnetization and their differences

N_{Co}	$E_{\text{SOC}}(\perp)$, eV	$E_{\text{SOC}}(\parallel)$, eV	ΔE_{SOC} , meV	E_{MA} , meV
1	−0.076661	−0.078297	1.636	0.898
2	−0.106206	−0.106064	−0.142	−0.062
3	−0.139079	−0.141456	2.377	1.161
4	−0.170703	−0.172107	1.403	1.098
5	−0.202876	−0.204850	1.974	1.032
6	−0.233835	−0.236287	2.452	1.525
7	−0.266121	−0.269110	2.986	1.760
8	−0.297662	−0.300837	3.176	2.040

cobalt monolayers. The inset in the main plot shows an approximation of the parameter of magnetic anisotropy, depending on the number of cobalt monolayers (except for $N_{\text{Co}} = 2$) on the logarithmic scale. Parameter $\lambda = 1.007$ was calculated as the angle of inclination of the approximation is similar to scaling parameter $\lambda = 1.02$ from [24]. The parameter of magnetic anisotropy disappears at a cobalt thickness of 2 monolayers, due to the change in the energy of magnetic anisotropy in both sign and value (Table 6). Raising the size of a surface cell (from 1 to 4 atoms in a layer) and the thickness of a nonmagnetic spacer (from 3 to 9 monolayers) did not eliminate this feature. In contrast to experiments, where partially filled layers were considered (i.e., the film thickness ranged from 1 to 2 monolayers with a step of 0.2), we considered the multiple thickness of a monolayer. Noncollinear calculations whose resource intensity depends strongly on the number of atoms in a supercell are required for determining magnetic anisotropy. With monolayers completely filled, it is sufficient to use 1 atom per layer, as we did in these calculations. With partially filled monolayers, we must take 4 or 9 atoms per layer, which raises the resource intensity of the calculation by an order of magnitude.

Table 5 gives the calculated average magnetic moments of the cobalt film for the same system. As in the collinear calculations (Table 3), we may conclude that different spin configurations affect the magnetic moments weakly. However, allowing for spin–orbit coupling in noncollinear calculations raises the magnetic moment and improves agreement with experiments.

The energy of magnetic anisotropy can be divided into two contributions: $E_{\text{MA}} = E_{\text{MCA}} + \Delta E_{\text{shape}}$ (MCA energy E_{MCA} induced by spin–orbit coupling) and ΔE_{shape} (the energy of shape anisotropy induced by magnetic dipole interactions). Contribution E_{MCA} is determined entirely by the electronic structure of the investigated system. It can be estimated directly from the spin–orbit coupling energy calculated for different

orientations of magnetization. the contribution is in this case $E_{\text{MCA}} = \Delta E_{\text{SOC}}$.

Table 6 compares the energies of spin–orbit coupling calculated with the VASP software package according to [25] at different directions of the magnetic moments. We can see that spin–orbit coupling was the main source of the MCA.

CONCLUSIONS

Results were presented from ab initio calculations of the magnetic properties of cobalt films separated by a nonmagnetic copper spacer. The energy efficiency of different spin configurations of such a trilayer system was examined and the magnetic moments at different layer thicknesses were obtained. The FM configuration became more energetically advantageous at three cobalt monolayers and spacer thicknesses of 5 and 9 monolayers (0.7 and 1.6 nm, respectively). The AFM configuration was favored at a copper thickness of 7 monolayers (~ 1.0 nm), as was confirmed experimentally in [13–15].

Magnetic moments of cobalt films of different thicknesses, obtained in both collinear and noncollinear calculations, showed that different spin configurations weakly affect the average values of the former. However, allowing for spin–orbit coupling in noncollinear calculations raises the magnetic moment and improves agreement with experiments. Calculations were made to describe the effect the surface orientation has on energy E_{MA} of magnetic anisotropy. They showed the direction of the magnetic moment parallel to the plane of the film is more energetically advantageous for faces (100) and (111). The existence of vanishingly weak anisotropy was established for face (110). The contributions from spin–orbit coupling to the energy of magnetic anisotropy were calculated.

The parameter of in-plane anisotropy depending on the number of cobalt monolayers will allow them to be used in Monte Carlo calculations of the coefficient of magnetoresistance.

ACKNOWLEDGMENTS

This work was performed with the computing resources of the shared resource center of the Far Eastern Branch of the Russian Academy of Sciences (Khabarovsk).

FUNDING

This work was supported by the Russian Science Foundation, project no. 23-22-00093.

CONFLICT OF INTEREST

The authors declare that they have no conflicts of interest.

REFERENCES

1. Heinrich, B. and Bland, J.A.C., *Ultrathin Magnetic Structures IV*, Berlin: Springer, 2005.
2. Shlyakhtich, M.A. and Prudnikov, P.V., *Bull. Russ. Acad. Sci.: Phys.*, 2023, vol. 87, no. 3, p. 389.
3. Prudnikov, V.V., Prudnikov, P.V., and Mamonova, M.V., *Phys.—Usp.*, 2017, vol. 60, p. 762.
4. Johnson, M.T., Bloemen, P.J.H., Broeder, F.J.A., and de Vries, J.J., *Rep. Prog. Phys.*, 1996, vol. 59, p. 1409.
5. Makeev, M.Yu. and Mamonova, M.V., *Bull. Russ. Acad. Sci.: Phys.*, 2023, vol. 87, no. 4, p. 427.
6. Kohlhepp, J., Elmers, H.J., and Gradmann, U., *J. Magn. Magn. Mater.*, 1992, vol. 111, p. 231.
7. Broeder, F.J.A., Hoving, W., and Bloemen, P.J.H., *J. Magn. Magn. Mater.*, 1991, vol. 93, p. 562.
8. Mushailov, E.S., Maltsev, V.K., Turpanov, I.A., and Kim, P.D., *J. Magn. Magn. Mater.*, 1994, vol. 138, p. 207.
9. Stearns, M.B. and Wijn, H.P.J., *Properties of Magnetic Materials*, Berlin: Landolt-Bornstein, 1986.
10. Hjortstam, O., Tyregg, J., Willis, J.M., Johansson, B., and Eriksson, O., *Phys. Rev. B*, 1996, vol. 53, p. 9204.
11. Wu, R. and Freeman, A.J., *J. Appl. Phys.*, 1996, vol. 79, p. 6500.
12. Daff, T.D. and de Leeuw, N.H., *J. Mater. Chem.*, 2012, vol. 22, p. 23210.
13. Ognev, A.V., Samardak, A.S., Vorob'ev, Yu.D., and Chebotkevich, L.A., *Phys. Solid State*, 2004, vol. 46, no. 6, p. 1084.
14. Chebotkevich, L.A., Vorob'ev, Yu.D., Samardak, A.S., and Ognev, A.V., *Phys. Solid State*, 2003, vol. 45, no. 5, p. 907.
15. Chebotkevich, L.A., Ognev, A.V., and Grudin, B.N., *Phys. Solid State*, 2003, vol. 46, no. 8, p. 1490.
16. Hjortstam, O., Tyregg, J., Willis, J.M., Johansson, B., and Eriksson, O., *Phys. Rev. B*, 1996, vol. 53, p. 9204.
17. Shick, A.B., Novikov, D.L., and Freeman, A.J., *Phys. Rev. B*, 1997, vol. 56, p. 561.
18. Pustogowa, U., Szunyogh, L., Ebert, H., and Weinberger, P., *Solid State Commun.*, 1998, vol. 108, p. 343.
19. Willis, R.F., Bland, J.A.C., and Schwarzacher, W., *J. Appl. Phys.*, 1998, vol. 63, p. 4051.
20. Kim, M., Freeman, A.J., and Wu, R., *Phys. Rev. B*, 1999, vol. 59, p. 9432.
21. Kuo, C.C., Lin, W.C., Chiu, C.L., et al., *J. Appl. Phys.*, 2001, vol. 89, p. 7153.
22. Shirinzadeh, H., *Int. J. Fundam. Phys. Sci.*, 2014, vol. 4, p. 89.
23. Kim, P.D., Chen, Yu.H., Turpanov, I.A., et al., *JETP Lett.*, 1996, vol. 64, no. 5, p. 370.
24. Huang, F., Kief, M.T., Mankey, G.J., et al., *Phys. Rev. B*, 1994, vol. 49, p. 3962.
25. Steiner, S., Khmelevskiy, S., Marsmann, M., and Kresse, G., *Phys. Rev. B*, 2016, vol. 93, p. 224425.

Translated by E. Bondareva